Tilt-Induced Changes in RR Series Characteristics: An AV Node Simulation Study

Felix Plappert[1], Mikael Wallman[2], Pyotr G Platonov[3], Sten Östenson[4], Frida Sandberg[1]

[1] Department of Biomedical Engineering, Lund University, Lund, Sweden
[2] Department of Systems and Data Analysis, Fraunhofer-Chalmers Centre, Gothenburg, Sweden
[3] Department of Cardiology, Clinical Sciences, Lund University, Lund, Sweden
[4] Department of Internal Medicine and Department of Clinical Physiology, Central Hospital Kristianstad, Sweden

Abstract

In the ECG recordings during tilt test, changes in RR series characteristics can be observed. The purpose of the present study is to investigate to what extent these changes can be explained by changes in the atrial input and in the atrioventricular (AV) nodal characteristics induced by the autonomic nervous system (ANS). Average RR series characteristics (mean, rmssd and sample entropy) and average atrial fibrillatory rate (AFR) were obtained from 24 patients during supine, head-down tilt (HDT), and head-up tilt (HUT). Simulations were performed using an AV node model consisting of a network of interacting node; each node with a refractory period (R) and conduction delay (D) dependent on the stimulation history. In an extension to the AV node model, R and D were scaled to account for ANS induced changes and simulations were performed with the original and extended model, respectively. The atrial impulse series entering the AV node was modelled as a point process with time-varying mean and std determined by the AFR. The clinical RR mean, RR rmssd and RR sample entropy decreased from supine to HDT and decreased further from HDT to HUT. Simulation results indicate that the model must account for ANS-induced changes to replicate the observed response in RR series characteristics, while alterations in the atrial input alone are insufficient to replicate the response.

1. Introduction

Atrial fibrillation (AF) is the most common supraventricular tachyarrhythmia affecting between 2% and 4% of the global population [1]. During AF, the atrial electrical activity and consequentially the heart rate is rapid and irregular. As AF poses a significant burden to patients, physicians and healthcare systems globally, the complex mechanisms of AF have to be better understood to personalize the treatment.

One contributor to the initiation and maintenance of AF is the autonomic nervous system (ANS) [2]. The autonomic tone in normal sinus rhythm is commonly quantified by heart rate variability (HRV) [3]. Results from previous studies on HRV suggest that ANS activity contributes to the initiation of episodes of paroxysmal atrial fibrillation [4]. Quantifying ANS activity during AF could allow for personalized treatment. The problem is that HRV is not applicable in AF as the ventricular rhythm is not initiated in the SA node. However, as the AV node is densely innervated by the ANS, the modulation of electrical impulses by the AV node could be utilized to quantify the autonomic tone. Therefore, investigating the complex AV nodal variations in electrophysiological properties may provide information about the ANS activity.

Fundamental to the AV nodal physiology are the slow pathway (SP) and fast pathway (FP) with different electrophysiological properties that are dynamic and depend on recently conducted and blocked impulses [5]. While the conduction delay is longer in the SP than in the FP, the refractory period is shorter. Several models of the AV node have been proposed previously, including earlier models that did not account for the dual-pathway physiology [6] as well as later models that accounted for separate refractory periods and conduction delays [7]. Crucially, the changes induced by the ANS have not been incorporated into the model description of previous models. Here, we are presenting an extension to a network model of the AV node, based on [8,9], that is modelling ANS-induced changes by scaling the refractory period and conduction delay. The complete study describing the AV node model extension is presented in [10]. The ANS-induced changes in heart rate and RR series variability and irregularity in patients with AF were evaluated using data from a head-up and head-down tilt test.

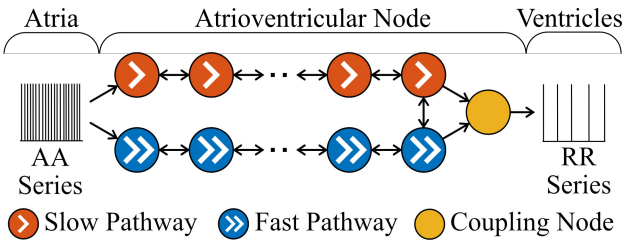

Figure 1. Illustration of the AV node model. Conduction within the model can be bidirectional. For simplicity, only a subset of the ten nodes in each pathway is shown.

2. Methods

2.1. Model Description

The presented AV node model was initially proposed in [8] with minor modifications in [9], and was extended to account for the effect of changes in the autonomic tone in [10]. The AV node is modelled by a network of 21 nodes (cf. Fig. 1). Each node represents a section of the AV node, where the slow pathway (SP) and fast pathway (FP) are described as chains of 10 nodes each. The last node of each chain is connected with one another and to an additional coupling node (CN). Atrial impulses enter at the first node of both pathways simultaneously; they can be conducted or blocked by a node and can leave the AV node over the CN resulting in a ventricular activation. Within both pathways and between the end nodes of the SP and FP, impulses can travel bidirectionally, allowing for retrograde conduction.

Each node is described with an individual refractory period $R^P(\Delta t_k, A_R)$ and conduction delay $D^P(\Delta t_k, A_D)$ defined as

$$R^P(\Delta t_k, A_R) = A_R \left(R^P_{min} + \Delta R^P \left(1 - e^{-\Delta t_k / \tau^P_R} \right) \right) \quad (1)$$

$$D^P(\Delta t_k, A_D) = A_D \left(D^P_{min} + \Delta D^P e^{-\Delta t_k / \tau^P_D} \right) \quad (2)$$

$$\Delta t_k = t_k - t_{k-1} - R^P(\Delta t_{k-1}, A_R), \quad (3)$$

where $P \in \{SP, FP, CN\}$ indicates the association to a pathway. If Δt_k is negative, the current node blocks the impulse due to the ongoing refractory period $R^P(\Delta t_{k-1}, A_R)$. If Δt_k is positive, the impulse is conducted and reaches all neighboring nodes after a delay determined by $D^P(\Delta t_k, A_D)$ and the current node is in refractory period for a time period determined by $R^P(\Delta t_k, A_R)$. Each node is characterized by eight parameters, defining the scaling of the refractory period by changes in the autonomic tone, A_R; minimum refractory period, R^P_{min}; maximum prolongation of refractory period, ΔR^P; time constant τ^P_R; scaling of the conduction delay by changes in the autonomic tone, A_D; minimum conduction delay, D^P_{min}; maximum prolongation of conduction delay, ΔD^P; and the time constant τ^P_D. The scaling factors A_R and A_D may change over time due to changes in the autonomic tone, while the other model parameters R^P_{min}, ΔR^P, τ^P_R, D^P_{min}, ΔD^P and τ^P_D remain fixed for a patient.

The impulse propagation through the AV node model is processed chronologically and node by node as described in detail in [8]. The incoming series of atrial impulses during AF is modelled as a point process with independent inter-arrival times distributed according to a Pearson Type IV distribution with a mean μ, standard deviation σ, skewness γ and kurtosis κ of the atrial activation (AA) series [11].

2.2. Tilt Test Study

The influence of the ANS on the RR series characteristics was investigated using ECG data recorded during a tilt test study reported in [12]. In the tilt test study, patients remained approximately 5 minutes in supine position, head-down tilt (HDT, -30°) and head-up tilt (HUT, 60°), respectively. The tilt test was performed between 1 pm and 3 pm in a quiet study room. ECG recordings from 24 patients with persistent AF were processed individually and the trend of the atrial fibrillatory rate (AFR) as well as the trends of the mean $\overline{RR}$, variability RR_V and irregularity RR_I of the RR series characteristics were computed. The RR series variability was quantified using the root mean square of successive RR interval differences (rmssd), and the RR series irregularity was quantified using the sample entropy [13] with $m = 2$ and $r = 0.2$. The AFR trends were used to estimate the trends of the AA series parameters, computed as the mean μ and standard deviation σ of 1/AFR. The AA series and RR series characteristic trends of the individual patients were averaged to obtain population-averaged trends of the AA series characteristics $\mu(t)$ and $\sigma(t)$ as well as the clinical population-averaged trends of the RR series characteristics $\overline{RR}^C(t)$, $RR^C_V(t)$ and $RR^C_I(t)$. A detailed description of the computation of the AA series and RR series characteristic trends can be found in [10].

2.3. Simulation

A set of 240 AV node model parameter vectors were used for the simulations with 10 parameter vectors per patient, selected based on their ability to replicate the RR series characteristics during supine. The selection process and the parameter sets are described in detail in [10]. To reduce the variability of results due to stochasticity, ten realizations were simulated for each of the 240 model parameter sets with a new realization of the AA series for each simulation. The AA series was modelled with a Pearson Type IV distribution using the estimated population-averaged $\mu(t)$ and $\sigma(t)$ trends, as well as fixed values

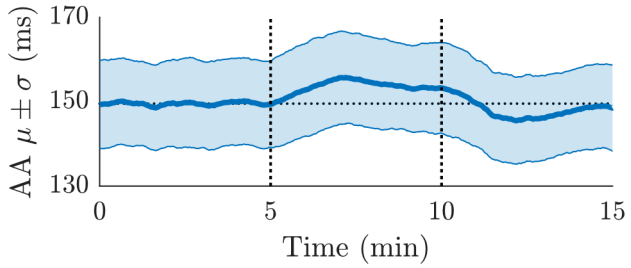

Figure 2. Estimated population-averaged mean and standard deviation trends of the AA series from ECG recording of 24 patients. The first five minutes were recorded in supine position, followed by five minutes in HDT and five minutes in HUT. The horizontal dotted line marks the averaged μ trend during the first five minutes.

for the skewness γ and kurtosis κ of 1 and 6, respectively. The γ and κ were fixed as they could not be estimated from the f-waves of the ECG. Simulations were performed for the original model [9] and extended model [10] using Eqs. (1)-(3). The original model does not include the scaling factors A_R and A_D, which is equivalent to A_R and A_D set to 1. In the extended model, the scaling factors had separate constant values for each tilt position and patient. The RR series characteristic trends were first computed for each simulation individually and then averaged to obtain the population-averaged trends of the original model $\overline{RR}^O(t)$, $RR_V^O(t)$ and $RR_I^O(t)$ and the extended model $\overline{RR}^E(t)$, $RR_V^E(t)$ and $RR_I^E(t)$, respectively.

3. Results

The estimated population-averaged $\mu(t)$ and $\sigma(t)$ trends are shown in Fig. 2. During supine position, $\mu(t)$ is approximately constant around 150 ms, while a clear variation is visible during tilt with $\mu(t)$ increasing during HDT and decreasing during HUT.

In Fig. 3, the population-averaged RR series characteristics $\overline{RR}^C(t)$, $RR_V^C(t)$ and $RR_I^C(t)$ are shown. $\overline{RR}^C(t)$ is significantly decreasing from supine to HDT and significantly decreasing further from HDT to HUT. $RR_V^C(t)$ and $RR_I^C(t)$ are decreasing from supine to HDT and decreasing further from HDT to HUT, showing a significant decrease from supine to HUT. Additionally, the population-averaged RR series characteristics of the original model $\overline{RR}^O(t)$, $RR_V^O(t)$ and $RR_I^O(t)$ and of the extended model $\overline{RR}^E(t)$, $RR_V^E(t)$ and $RR_I^E(t)$ are shown. For the simulated RR series characteristic trends of the extended model shown in Fig. 3, the scaling factors were set to $A_R = 1$ and $A_D = 1$ during supine position, $A_R = 1$ and $A_D = 0.9$ during HDT and $A_R = 0.95$ and $A_D = 0.9$ during HDT. Similar to the clinical data, the $\overline{RR}^E(t)$, $RR_V^E(t)$ and $RR_I^E(t)$ are decreasing from supine to HDT and decreasing further from HDT to HUT. In contrast, the $\overline{RR}^O(t)$, $RR_V^O(t)$ and $RR_I^O(t)$ are decreasing from supine to HDT, but increasing from HDT to HUT. The RR series irregularity trends show that the sample entropy of the simulated RR series $RR_I^O(t)$ and $RR_I^E(t)$ are lower compared to the clinical RR series $RR_I^C(t)$, implying that the AV node model output is generally too regular.

4. Discussion and Conclusion

Our results (Fig. 3) show that the extended model, unlike the original model, can replicate the observed changes in the clinical RR series characteristics during HDT and HUT. When using the original model, the changes in atrial activity observed from the f-waves of the ECG are incorporated, but not the ANS-induced scaling of the refractory period and conduction delay. This causes $\overline{RR}^O(t)$, $RR_V^O(t)$ and $RR_I^O(t)$ to increase from HDT to HUT, which is the opposite direction of change of $\overline{RR}^C(t)$, $RR_V^C(t)$ and $RR_I^C(t)$ (Fig. 3). Conversely, the observed changes in $\overline{RR}^C(t)$, $RR_V^C(t)$ and $RR_I^C(t)$ could be replicated by the extended model (Fig. 3). The scaling factors $A_R = 1$ and $A_D = 0.9$ for HDT and $A_R = 0.95$ and $A_D = 0.9$ for HUT were selected based on their ability to replicate the observed changes in clinical RR series characteristics. Results with several values for the scaling factors A_R and A_D are presented in [10]. It should be noted that similar changes in RR series characteristics can be obtained with other scaling factors. These results suggest that the changes in RR series characteristics observed during tilt-test are largely resulting from ANS-induced changes in AV nodal conduction properties. The presented extension to the AV node model using scaling factors for the refractory period and conduction delay does not distinguish between changes induced by the sympathetic nervous system and changes induced by the parasympathetic nervous system. Instead, the scaling factors A_R and A_D are modelling the joint effect of changes in sympathetic and parasympathetic activity.

When comparing $RR_I^O(t)$ and $RR_I^E(t)$ with $RR_I^C(t)$, the simulated RR series are more regular than the clinical RR series, indicated by a lower sample entropy. One possible cause of the lower irregularity in the simulated RR series may be the static description of the AV nodal refractoriness and conduction delay. It would be interesting to evaluate if the addition of short-term variation in AV nodal refractoriness and conduction delay to the AV node model is increasing the RR series irregularity. Such short-term variation may originate from respiratory modulation in the ANS activity, and could be incorporated in the model via periodical variations in A_R and A_D.

We present an extension to an AV node model that is ac-

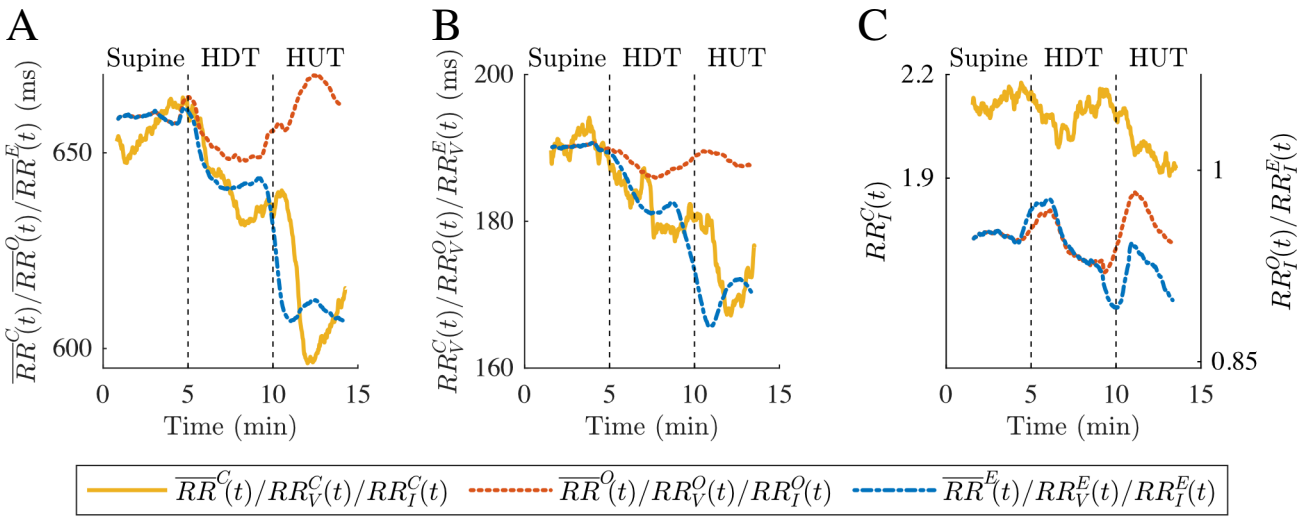

Figure 3. Average clinical RR series characteristics (A) $\overline{RR}^C(t)$, (B) $RR_V^C(t)$ and (C) $RR_I^C(t)$ (yellow) and average simulated RR series characteristics for the original model (A) $\overline{RR}^O(t)$, (B) $RR_V^O(t)$ and (C) $RR_I^O(t)$ (red) and average simulated RR series characteristics for the extended model (A) $\overline{RR}^E(t)$, (B) $RR_V^E(t)$ and (C) $RR_I^E(t)$ (blue). The dashed black lines separate the five minute segments of supine, HDT and HUT, respectively.

counting for ANS-induced changes. Further, we demonstrate the necessity of the model extension to replicate tilt-induced changes in heart rate and RR series variability and irregularity.

Acknowledgments

The research was supported by the Swedish Research Council (grant VR 2019–04272) and the Crafoord Foundation (grant 20200605). The computations were enabled by resources provided by the Swedish National Infrastructure for Computing (SNIC) at Lund University partially funded by the Swedish Research Council through grant agreement no. 2018-05973.

References

[1] Hindricks G et al. 2020 ESC Guidelines for the diagnosis and management of atrial fibrillation developed in collaboration with the European Association for Cardio-Thoracic Surgery (EACTS). Eur Heart J 2020;42(5):1–126.

[2] Shen MJ and Zipes, Douglas P. Role of the autonomic nervous system in modulating cardiac arrhythmias. Circ Res 2014;114(6):1004–1021.

[3] Sassi R et al. Advances in heart rate variability signal analysis: joint position statement by the e-Cardiology ESC Working Group and the European Heart Rhythm Association co-endorsed by the Asia Pacific Heart Rhythm Society. EP Europace 2015;17(9):1341–1353.

[4] Lombardi F et al. Autonomic nervous system and paroxysmal atrial fibrillation: A study based on the analysis of RR interval changes before, during and after paroxysmal atrial fibrillation. Eur Heart J 2004;25(14):1242–1248.

[5] George SA et al. At the atrioventricular crossroads: dual pathway electrophysiology in the atrioventricular node and its underlying heterogeneities. Arrhythmia Electrophysiol Rev 2017;6(4):179–185.

[6] Cohen, RJ et al. A quantitative model for the ventricular response during atrial fibrillation. IEEE Trans Biomed Eng 1983;30(12):769–781.

[7] Inada S et al. Simulation of ventricular rate control during atrial fibrillation using ionic channel blockers. J Arrhythm 2017;33(4):302–309.

[8] Wallman, M and Sandberg, F. Characterisation of human AV-nodal properties using a network model. Med Biol Eng Comput 2018;56(2):247–259.

[9] Karlsson M et al. Non-invasive characterization of human AV-nodal conduction delay and refractory period during atrial fibrillation. Frontiers in Physiology 2021;12.

[10] Plappert F et al. An atrioventricular node model incorporating autonomic tone. Front Physiol 2022;13.

[11] Climent AM et al. Generation of realistic atrial to atrial interval series during atrial fibrillation. Med Biol Eng Comput 2011;49(11):1261–1268.

[12] Östenson S et al. Autonomic influence on atrial fibrillatory process: Head-up and head-down tilting. Ann Noninvasive Electrocardiol 2017;22(e12405).

[13] Richman, JS and Randall Moorman, J. Physiological time-series analysis using approximate entropy and sample entropy. Am J Physiol Heart Circ Physiol 2000;278(6):2039–2049.

Address for correspondence:

Felix Plappert
Lund University, Department of Biomedical Engineering
Box 118, 221 00 Lund, Sweden
felix.plappert@bme.lth.se